

## Article

# Unravelling Nutrients and Carbon Interactions in an Urban Coastal Water during Algal Bloom Period in Zhanjiang Bay, China

Jibiao Zhang <sup>1</sup>, Miaojian Fu <sup>1</sup>, Peng Zhang <sup>1,2,\*</sup>, Dong Sun <sup>1,2</sup> and Demeng Peng <sup>1</sup><sup>1</sup> College of Chemistry and Environmental Science, Guangdong Ocean University, Zhanjiang 524088, China<sup>2</sup> Research Center for Coastal Environmental Protection and Ecological Resilience, Guangdong Ocean University, Zhanjiang 524088, China

\* Correspondence: zhangpeng@gdou.edu.cn; Tel.: +86-0759-2383300

**Abstract:** Nutrients and carbon play important roles in algal bloom and development. However, nutrients and carbon interactions in the period of the spring algal bloom are not well understood. The aim of this study is to explore the nutrients and carbon interactions in the period of the spring algal bloom covering an urban Jinsha Bay (JSB) coastal water in Zhanjiang Bay (South China Sea) using in situ multidiscipline observation. The results showed that the average concentration of total nitrogen (TN), total phosphorus (TP), and dissolved silicon (DSi) was  $97.79 \pm 26.31 \mu\text{mol/L}$ ,  $12.84 \pm 4.48 \mu\text{mol/L}$ , and  $16.29 \pm 4.00 \mu\text{mol/L}$  in coastal water, respectively. Moreover, the average concentration of total dissolved carbon (TDC), dissolved inorganic carbon (DIC) and organic carbon (DOC) in JSB was  $2187.43 \pm 195.92 \mu\text{mol/L}$ ,  $1516.25 \pm 133.24 \mu\text{mol/L}$ , and  $671.13 \pm 150.81 \mu\text{mol/L}$ , respectively. Furthermore, the main dominant species were *Phaeocystis globosa* and *Nitzschia closterium* during the spring algal bloom. Additionally, the correlation analysis showed salinity (S) was significantly negatively correlated with nutrients, indicating that nutrients derived from land-based sources sustained spring algal bloom development. However, as the major fraction of TDC, DIC was significantly positively correlated with S, which was mainly derived from marine sources. Besides, the algal density showed a significant positive correlation with temperature (T) ( $p < 0.001$ ) and dissolved oxygen (DO) ( $p < 0.001$ ), but a significant negative correlation with DIC ( $p < 0.05$ ), suggesting that spring algal blooms may be simulated by water T increase, and then large amounts of DIC and nutrients were adsorbed, accompanying DO release through photosynthesis in coastal water. This study revealed nutrients and carbon interactions in the spring algal bloom of urban eutrophic coastal water, which has implications for understanding the nutrients and carbon biogeochemical cycle and algal bloom mitigation under climate change and anthropogenic pressures in the future.

**Keywords:** nutrients; carbon; speciation; algal bloom; eutrophication; coastal water

check for updates

**Citation:** Zhang, J.; Fu, M.; Zhang, P.; Sun, D.; Peng, D. Unravelling Nutrients and Carbon Interactions in an Urban Coastal Water during Algal Bloom Period in Zhanjiang Bay, China. *Water* **2023**, *15*, 900. <https://doi.org/10.3390/w15050900>

Academic Editors: Michael Karydis and Maurizio Azzaro

Received: 19 January 2023

Revised: 19 February 2023

Accepted: 24 February 2023

Published: 26 February 2023



**Copyright:** © 2023 by the authors. Licensee MDPI, Basel, Switzerland. This article is an open access article distributed under the terms and conditions of the Creative Commons Attribution (CC BY) license (<https://creativecommons.org/licenses/by/4.0/>).

## 1. Introduction

Nutrients, including nitrogen (N), phosphorus (P), and silicon (Si), are the indispensable nutrient substances in the ocean environment and the driving force behind primary productivity, which is essential for the growth, development and reproduction of organisms [1–6]. Phytoplankton are often regarded as the basis for maintaining and influencing matter cycling and energy flow in aquatic systems. Changes in nutrient concentration and composition are closely linked to biogeochemical processes and significantly affect phytoplankton community structure and primary productivity [7–9]. In seawater, dissolved inorganic phosphorus (DIP) and dissolved inorganic nitrogen (DIN) are the most effective forms absorbed by phytoplankton [10]. In addition, it has been found that dissolved organic nitrogen (DON) can also be absorbed by phytoplankton in coastal ecosystems to form algal blooms [11], but for different species of algal blooms, the ability to absorb DON is different [12]. While phytoplankton occurs in coastal algal blooms, N is the limiting

nutrient that mainly controls the growth of phytoplankton, which responds very rapidly to DIN, and primary productivity increases rapidly in a few days under sufficient DIN; while P is the ultimate limiting nutrient that regulates primary productivity in the ocean on long time scales [13]. Carbon in seawater exists in various forms, including DIC, DOC, and particulate organic carbon (POC), among which DIC is one of the elements directly used by phytoplankton and bacteria for photosynthesis and is closely related to atmospheric CO<sub>2</sub> concentration [14–16]. In addition, the main source of DOC is ascribed to the action of organisms which is related to primary productivity [17–19]. Phytoplankton photosynthesis absorbs C, N, P to form organic matter and release oxygen. In turn, the remineralization of the algae process changes organic matter into DIC, forming a carbon cycle [18,20].

In the last decades, with rapid population growth and economic development of coastal areas, the effect of land-based sources of pollutants on the marine environment has become more and more serious, such as with the increase of agricultural wastewater, farming wastewater, urban wastewater, and industrial wastewater [21–24]. Many coastal and estuarine areas are also being enriched with nutrients and are becoming increasingly eutrophic [21,25–27]. As a result, nutrients composition and stoichiometry of coastal areas have changed significantly, and a serious consequence of this imbalance is that the water body is in over-eutrophication, which promotes catastrophic marine ecological phenomena, such as red tides, green tides, ocean anoxia, and acidification [9,28]. On the other hand, phytoplankton is also a key part of the biological pump, which not only affects the nutrients distribution in local waters, but also affects the carbon cycle in the coastal ecosystem [29]. Occurrences of algal blooms are influenced by a number of processes, including physical, chemical, and biological reactions, but the mechanisms of spring algal blooms occurrence are not fully understood [11,30]. Previous studies have shown that coastal temperature plays an important role in green tide blooms in the Yellow Sea and coastal red tides in the East China Sea [31,32]. In addition, artificial stress has led to a significant increase in nutrient status in the Zhanjiang Bay over the past three decades. The coastal water has shifted from a P-limited oligotrophic state before the 2000s to an N-limited eutrophic state [33]. Besides, in a study of the Yangtze estuary, nutrients input was found to be a factor in the occurrence of algal blooms [34]. Moreover, the previous study also found the important role of green tide (*Ulva prolifera*) blooms in the dissolved organic matter (DOM) pool and its significant effect on the marine carbon cycle [35]. However, changes in the carbonate system during algal blooms have less impact on the climate and the algal bloom of different types of phytoplankton is not only related to environmental factors, but also closely related to different driving effects of nutrients and carbon on algal blooms in different regions around the world [36,37]. The interactions between nutrients and carbon during spring algal blooms were also difficult to understand and the environmental factors, such as nutrients and temperature in offshore seawater, were affected by the tidal hydrological conditions [23]. Therefore, it may be difficult to carry out the field measurement of a wide range of observation stations and multiple parameters in a short time. However, the study of carbon and nutrients during spring algal blooms in a short-term period is scarce at present. Outbreaks of algal blooms have a significant impact on the physicochemical properties of the seawater, biogeochemistry of nutrients and carbon, such as uptaking and releasing, as well as the abundance and species composition of phytoplankton. Therefore, in situ multidisciplinary observations of environmental factors, nutrient status, and carbon pools during algal bloom development were conducted to fully understand the biogeochemical interaction mechanism and speciation of carbon and nutrients during the occurrence of spring algal blooms.

Jinsha Bay (JSB) is an inner part of the Zhanjiang Bay, which is a typical semi-enclosed bay [38]. In recent years, with the growing population and rapid economic development in Zhanjiang city, the pollution from land-based sources, such as domestic and farming wastewater into the bay through rivers and outfalls, has become more and more serious, leading to the deterioration of seawater quality and the increase of eutrophication [38]. According to the national seawater quality standards of China, seawater with inorganic

nitrogen exceeding 35.71  $\mu\text{mol/L}$  and inorganic phosphorus exceeding 1.29  $\mu\text{mol/L}$  is categorized as inferior Class IV seawater. The nitrogen and phosphorus levels in the seawater of Zhanjiang have long exceeded Class IV seawater quality standards [38,39]. In addition, algal blooms rarely occurred before the 1980s but have occurred periodically and frequently since the 2000s. The spring season was identified as the most frequent blooming period [33]. However, nutrients and carbon interactions were not well understood during the spring algal bloom period, which makes it hard to mitigate algal blooms under climate change and anthropogenic pressures in the future. In spring 2022, algal blooms began to appear near JSB coastal water, which provided us with a good experimental site for clarifying nutrients and carbon interactions in the algal bloom of JSB coastal water.

Therefore, nitrogen, phosphorus, dissolved carbon, and phytoplankton species in the coastal water during the algal blooms period in the spring season, 2022, were measured using the in situ multidiscipline observation and laboratory analysis to: (1) explore the nutrients and carbon distribution; (2) identify the main phytoplankton species in the algal bloom; (3) clarify the relationships among nutrients, carbon, and phytoplankton during the spring algal bloom period. Therefore, this study revealed the nutrients and carbon interactions in the spring algal bloom of JSB coastal water, which provided implications for understanding the nutrients and carbon biogeochemical cycle and algal bloom mitigation under climate change and anthropogenic pressures in the future.

## 2. Materials and Methods

### 2.1. Study Area

Zhanjiang Bay is located in the southernmost mainland of China. As a part of Zhanjiang Bay (Figure 1A), JSB is located on the east coast of Chikan District, Zhanjiang City, covering an area of 126,000 square meters as part of Zhanjiang Bay. It is a recreational and scenic area owing to a large natural seaside bathing area with many visitors and a large Binhu Park of more than 400 acres on the top of JSB. Because of the special geographic features of JSB's inner concave coastline, it can reduce the wave intensity from the mouth of Zhanjiang Bay to JSB to a certain extent. Moreover, the beach of JSB is wave-gentle with rather fine sand, which is very suitable as a beach bathing place. The surrounding environment of JSB is favorable for tourism and recreation due to specific coastal characteristics and high ecological value. As a famous scenic spot, its unique marine scenery attracts tourists from home and abroad with over 100,000 people each year. In recent decades, with the rapid development of the city space and population, the rapid expansion of aquaculture and industry, eutrophication of sewage has occurred through the rivers and outfalls into the JSB [40]. However, since 2005, there have been 1–2 algal blooms in ZJB almost every year, and the frequency of occurrence and the area of the bloom have shown a fluctuating trend [33]. The water quality of JSB has caused some harmful effects, such as making the JSB water body show a state of eutrophication and easily triggering algal blooms. It also endangers the health of visitors to the beach baths. Above-mentioned harmful influences have resulted in a sharp drop of the tourism and ecological value of JSB [33].

### 2.2. Field Monitoring Stations and Sampling

In this study, the inshore investigation of the whole JSB was carried out. Taking the southmost of JSB as the base point, five section lines were set with a 50-m span between two adjacent lines, and about a 50-m span was arranged between two adjacent stations in the same section line (Figure 1B). To investigate the impact on the coastal environment of JSB during the spring algal blooms, surface water samples were collected from the coastal seawater of JSB at each site. Because the water area of JSB was the largest during high tide and best reflects the environmental characteristics of JSB, and considering that at low tide time, the seawater was already far away from the area in JSB where people were closely connected with the environment, therefore a semidiurnal tide with a period of 12 h at high tide was chosen as the field survey period, with an average water depth of the station at about 2 m. (Figure 1C). Fieldwork during the spring algal blooms was

conducted at JSB during the high tide period from 11:00 to 13:00 on 19 March 2022. To avoid the hydrodynamic effects of the tide on spring algal blooms, samples of seawater were collected simultaneously at JSB within 2 h of high tide. Surface seawater (0.5 m) was taken using an unmanned sampling boat (YUNZHOU SS20). Seawater samples were kept in polyethylene bottles and were taken back to the laboratory within 0.5 h. The original and filtered water samples were frozen in the refrigerator at  $-20\text{ }^{\circ}\text{C}$  for future use.

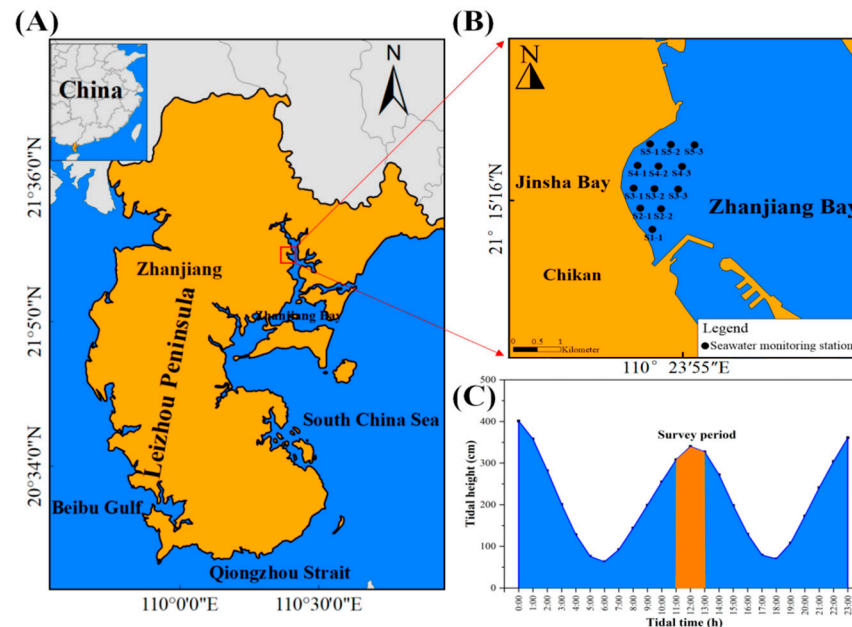


**Figure 1.** Geographical location of Zhanjiang Bay (ZJB) (A), Jinsha Bay (B), and tidal variation in ZJB (C).

### 2.3. Analytical Method

The experimental samples were obtained in the JSB spring algal blooms period on March 19. DO, T, pH, and Salinity (S) were determined in situ by multi-parameter water quality analyzers (AQUAREAD AP7000) while sampling. Twelve seawater samples were collected [41] and they were kept frozen at  $-20\text{ }^{\circ}\text{C}$  before chemical analysis. After sample collection, acid-precleaned  $0.45\text{ }\mu\text{m}$  cellulose acetate filters were used to filter the samples, which were rinsed with pure water before use [42]. In this study, the DIN concentration included the  $\text{N-NO}_3^-$ ,  $\text{N-NO}_2^-$ , and  $\text{N-NH}_4^+$  species, and the  $\text{P-PO}_4^{3-}$  was regarded as DIP. In the laboratory analysis, the DIN and DIP in JSB were determined by the standard colorimetric methods as described in the Specification of Oceanographic Survey [42]. Inorganic phosphorus was analyzed by the phosphorus-molybdenum blue method (SHIMADZU, UV-2600i) with a minimum detection limit of  $0.32\text{ }\mu\text{mol/L}$ . Total phosphorus was analyzed by the potassium persulphate oxidation method with a minimum detection limit of  $0.32\text{ }\mu\text{mol/L}$ ; nitrite was analyzed by the diazo coupling method with a minimum detection concentration of  $0.21\text{ }\mu\text{mol/L}$ ; nitrate was analyzed by the zinc-cadmium reduction method with a minimum detection concentration of  $0.21\text{ }\mu\text{mol/L}$ ; ammonium was analyzed by the hypobromite oxidation method with a minimum detection concentration of  $0.36\text{ }\mu\text{mol/L}$ . TN was determined using an oxidation method with a minimum detection concentration of  $0.21\text{ }\mu\text{mol/L}$ . DSi was detected by silicon-molybdenum blue spectrophotometry with a minimum detection concentration of  $0.67\text{ }\mu\text{mol/L}$  [43]. TDC, DOC, and DIC were determined via catalytic high-temperature oxidation using a total organic carbon analyzer (TOC-L CPH/CPN, Shimadzu Co., Kyoto, Japan) with a platinum catalyst at  $680\text{ }^{\circ}\text{C}$  using a non-dispersive infrared gas analyzer. Its minimum detection concentration was  $3.3\text{ }\mu\text{mol/L}$  [44]. Lugol's iodine solution was added immediately after collecting 500 mL of phytoplankton samples, and the supernatant liquid was removed

and concentrated to 100 mL after 48 h of natural settling [45]. After the samples were shaken well, three 100  $\mu$ L concentrated subsamples of each water sample were placed in a counting frame, counted using a microscope (SDPTOP, EX30) and averaged, and the phytoplankton biodensities were obtained by multiplying the concentration multiplier after counting. Species identification was performed by bibliographic reference, and the degree of the algal bloom was graded according to the Technical Specification for Classification and Monitoring of Algal Blooms [46–48]. The precision was estimated to be better than 5% by repeated determination of 10% of the samples. In each batch of samples, the standard solution from the Institute of Standard Samples of the Ministry of Environmental Protection of The People’s Republic of China was used as the quality control sample to ensure the accuracy of test results (96–103%).

#### 2.4. Statistical Method

The geographic information system ArcGIS (10.2) was used to map the monitoring stations of the JSB coastal water. Using Origin (2021), the spatial and temporal distributions of C, N, P, DSi and algal density were plotted, using weighted average grid interpolation. The Hierarchical Clustering method was used to map the genealogy of dominant species with respect to the station. The CANOCO 5.0 (Microcomputer Power, USA) was used to explore the relationship between environmental factors and two species of algae. The Shannon–Weaver index ( $H'$ ) and dominance ( $Y$ ) was calculated according to the following equation.

$$H' = - \sum_{i=1}^s P_i \log_2 P_i \quad (1)$$

$$Y = \frac{n_i}{N} f_i \quad (2)$$

where ( $s$ ) is the total number of species in the sample; ( $P_i$ ) is the ratio of the number of individuals of the  $i$ th species ( $n_i$ ) to the total number of individuals ( $N$ ), ( $f_i$ ) indicates the frequency of the species at each sampling site, and when  $Y > 2$ , the species is the dominant species in the community. Correlation analysis was used and plotted to analyze the relationships among environmental indicators, nutrients, carbon, and phytoplankton,  $p < 0.05$  for statistically significant difference. The data were analyzed by Excel 2020 software, and the data were expressed as arithmetic (Mean  $\pm$  SD).

### 3. Results

#### 3.1. Environmental Condition of Coastal Water during the Spring Algal Bloom Period

During the accumulating phase of the algal bloom, the T in the JSB coastal water fluctuated from 27.0  $^{\circ}$ C to 28.5  $^{\circ}$ C, with an average of 27.74  $\pm$  0.54  $^{\circ}$ C, T decreases with increasing distance from the coast (Table 1). The pH ranged from 7.74 to 8.52, with an average of 8.25  $\pm$  0.22, and it showed a decreasing gradient from the nearshore to the farshore in the JSB coastal water. In addition, the concentration of DO fluctuated between 7.48–8.10 mg/L, with an average concentration of 7.82  $\pm$  0.18 mg/L. DO showed a similar spatial distribution pattern as pH. Besides, the S fluctuated from 11.8 PSU to 23.9 PSU, with an average of 16.73  $\pm$  4.31 PSU. During the high tide survey in JSB, the seawater dynamics were evident and showed significant differences in spatial salinity, exhibiting low S near the shore and high S away from shore. Additionally, the concentration of total dissolved particulate (TSP) averaged 41.18  $\pm$  14.27 mg/L, ranging from 19.2 mg/L to 73.8 mg/L.

**Table 1.** Environmental condition of coastal water during the spring algal bloom period.

Station	T (°C)	pH	DO (mg/L)	S (PSU)	TSP (mg/L)
S1-1	28.2	7.74	7.93	16.5	60.2
S2-1	28.3	7.97	7.94	15.5	50.6
S3-1	28.4	8.43	7.95	12.2	45.8
S4-1	28.3	8.52	8.01	11.8	73.8
S5-1	28.5	8.50	8.10	12.2	41.0
S2-2	27.6	8.16	7.82	17.9	28.8
S3-2	27.3	8.15	7.48	23.9	35.6
S4-2	27.7	8.41	7.79	11.8	37.6
S5-2	27.1	8.26	7.64	21.7	37.4
S3-3	27.2	8.37	7.83	14.8	19.2
S4-3	27.3	8.32	7.73	18.9	27.2
S5-3	27.0	8.14	7.56	23.5	37.0

### 3.2. Spatial Nutrients Distribution in the JSB Seawater

During the investigation period, the concentration of  $\text{N-NO}_2^-$  in the JSB surface water was low and relatively uniform from coast to offshore (Figure 2A). In addition, the average  $\text{N-NH}_4^+$  concentration in JSB was high in the offshore and low in the coast (Figure 2C).  $\text{N-NO}_3^-$  as a major speciation of DIN, the concentration of  $\text{N-NO}_3^-$  shows a characteristic of high on the coast and low offshore and reached a maximum of  $52.10 \mu\text{mol/L}$  at S3-1 (Figure 2B). In addition, the concentration of the DIN distribution pattern in general was similar to that of  $\text{N-NO}_3^-$  (Figure 2D). The distribution of dissolved organic nitrogen (DON) concentrations was not uniform, with low concentrations occurring in the middle of the survey area (Figure 2E). In addition, the concentration of total dissolved nitrogen (TDN) fluctuated in a small range and showed a maximum of  $109.36 \mu\text{mol/L}$  at S1-1 (Figure 2F). Additionally, the concentration of PN showed a maximum of  $52.71 \mu\text{mol/L}$  at S4-2, but overall, it still showed high on the coast and low offshore (Figure 2G). The concentration of TN distribution characteristics was similar to PN and showed a maximum of  $135.07 \mu\text{mol/L}$  at S4-2 (Figure 2H). DIN was the major fraction nutrients form of N in JSB. In addition, the concentration of DIP in the JSB surface water shows a characteristic of high on the coast and low offshore (Figure 2I). Furthermore, dissolved organic phosphorus (DOP) only occurs in S5-1 with a high concentration of  $9.76 \mu\text{mol/L}$ , while the rest of the area had low concentrations and uniform distribution (Figure 2J). Moreover, the concentration of total dissolved phosphorus (TDP) showed an overall higher near-shore than farshore characteristic (Figure 2K), and the maximum of  $14.07 \mu\text{mol/L}$  occurred at the S3-1 in the middle of the sea. Besides, the concentration distribution of particulate phosphorus (PP) was uniform (Figure 2L). The concentration of total phosphorus (TP) was similar to DIP concentration distribution (Figure 2M), and DIP was the major fraction nutrients form of P in JSB. Additionally, the dissolved silicon (DSi) concentrations were higher in the coastal waters adjacent to the beach and decreased extending seaward; the highest concentration occurred at S3-1 as  $21.55 \mu\text{mol/L}$  (Figure 2N).

### 3.3. Spatial Carbon Speciation Distribution and Composition in the JSB Seawater

The concentration of DOC in the JSB surface water was only higher in S3-1 at  $1010.83 \mu\text{mol/L}$  and was more evenly distributed in other areas (Figure 3A). Furthermore, the average DIC was evenly distributed in JSB coastal water (Figure 3B). Additionally, the concentration of TDC shows a characteristic of high on the coast and low offshore, the maximum value of the concentration occurred in S3-1 and was  $2471.67 \mu\text{mol/L}$  (Figure 3C). The distribution of TDC changed relatively small in the study area, and the DOC and DIC accounted for 30.4% and 69.5%, respectively. Besides, the composition of DOC and DIC was remarkably different in spatial distribution (Figure 3D), and the proportion of DOC nearshore was larger than the coastal water.

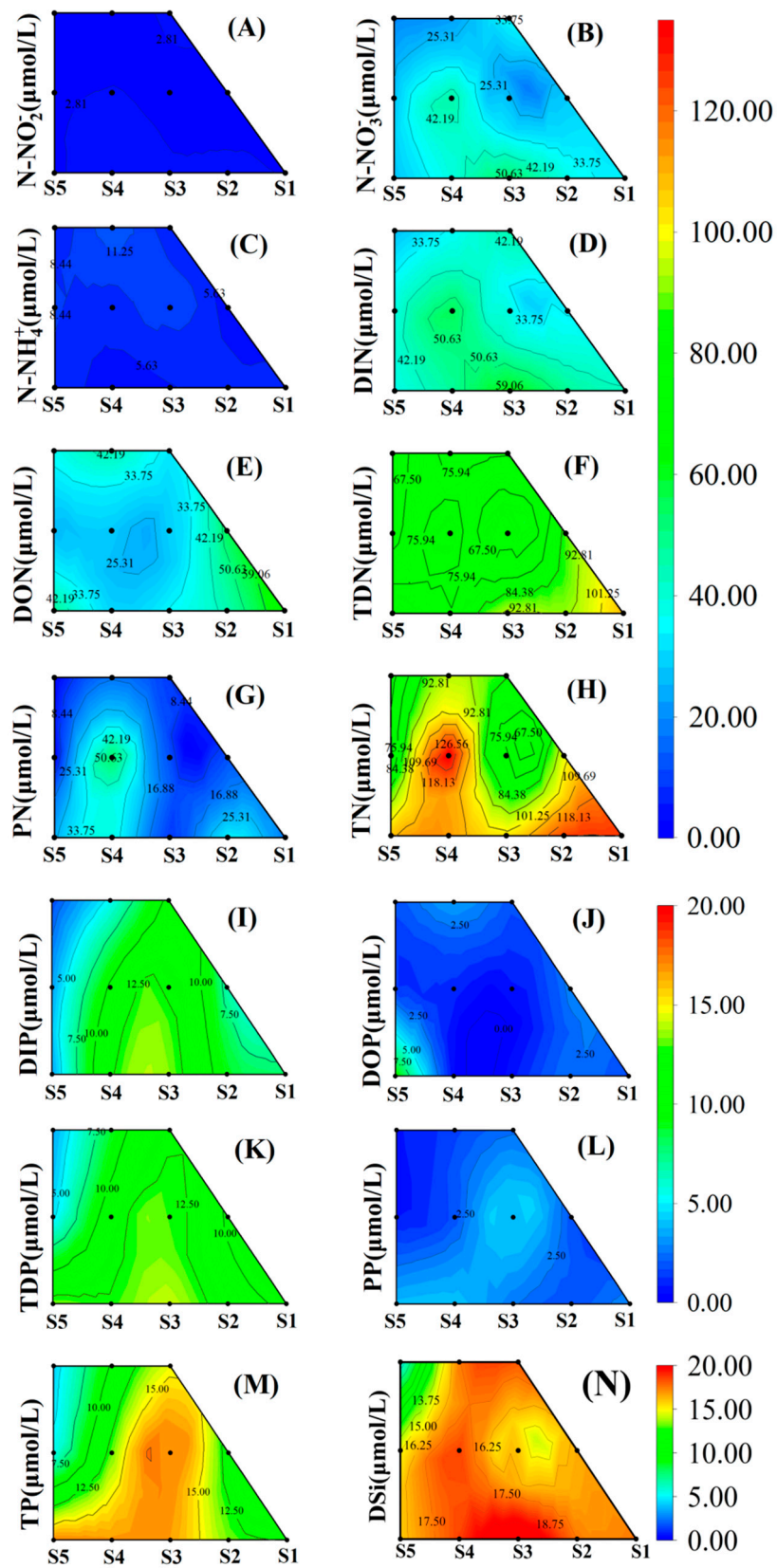


**Figure 2.** Spatial distribution of  $N-NO_2^-$  in JSB (A), spatial distribution of  $N-NO_3^-$  in JSB (B), spatial distribution of  $N-NH_4^+$  in JSB (C), spatial distribution of DIN in JSB (D), spatial distribution of DON in JSB (E), spatial distribution of TDN in JSB (F), spatial distribution of PN in JSB (G), spatial distribution of TN in JSB (H), spatial distribution of DIP in JSB (I), spatial distribution of DOP in JSB (J),

spatial distribution of TDP in JSB (K), spatial distribution of PP in JSB (L), spatial distribution of TP in JSB (M), and spatial distribution of DSi in JSB (N).

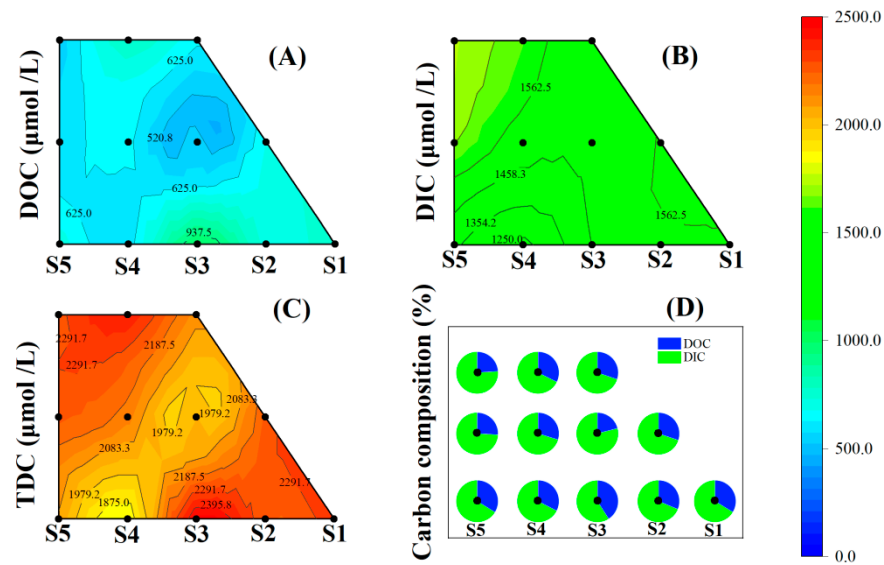


**Figure 3.** Spatial distribution of DOC in JSB coastal waters (A), spatial distribution of DIC in JSB coastal waters (B), spatial distribution of TDC in JSB coastal waters (C), and the percentage of DOC and DIC in JSB coastal waters (D).

### 3.4. Spatial Phytoplankton Density in the JSB Coastal Water during Spring Algal Bloom

The phytoplankton of JSB was enriched at the shore and the concentration gradually decreased towards the coastal water. Algal density averaged  $(2.20 \pm 1.24) \times 10^6$  cells/mL, ranging from  $1.18 \times 10^5$  cells/mL to  $4.18 \times 10^6$  cells/mL, reaching the level of V algal bloom (Figure 4A) [47]. Nine phytoplankton species were found in the sampling stations, with a Shannonville index of 1.03. Except for two dominant species that were mainly present, the number of other phytoplankton species was very small. The main dominant species in each station in JSB waters were *P. globosa*, the secondary dominant species were *N. closterium*, and in the S5-3, there was additionally *Skeletonema* (Figure 4B). The total densities of the main and secondary dominant species were  $(1.14 \pm 0.689) \times 10^6$  cells/mL and  $(1.05 \pm 0.634) \times 10^6$  cells/mL, respectively, and the degrees of dominance were 0.52 and 0.48, respectively. The systematic clustering analysis also showed that the nearshore and far-shore were divided into two groups (Figure 5). In addition, the results showed that the distribution of algae showed remarkably spatial differences, which was that the algal density in the nearshore was significantly higher than that in the farshore.

### 3.5. Relationships among Nutrients, Carbon and Phytoplankton during Spring Algal Bloom

The relationships among nutrients, carbon, and phytoplankton in the JSB during the spring algal bloom were shown (Figure 6). The results showed that algal density and T showed a significant positive correlation ( $p < 0.001$ ), but significantly negatively correlated with S. Moreover, a significant positive correlation ( $p < 0.001$ ) was found between algal density and DO. In addition,  $\text{N-NO}_2^-$  ( $p < 0.01$ ),  $\text{N-NO}_3^-$  ( $p < 0.001$ ), DIN ( $p < 0.01$ ), PN ( $p < 0.01$ ), TN ( $p < 0.01$ ), DSi ( $p < 0.01$ ), and S showed a significant positive correlation. Besides, algal density was positively and significantly correlated ( $p < 0.05$ ) with DIN, but insignificantly correlated with DIP. Algal density was positively and significantly correlated ( $p < 0.05$ ) with DOC, but negatively and significantly correlated ( $p < 0.05$ ) with DIC. Additionally,  $\text{N-NO}_2^-$  ( $p < 0.01$ ),  $\text{N-NO}_3^-$  ( $p < 0.001$ ), and DIN showed a significant positive correlation. It was also found that both *P. globosa* and *N. closterium* had approximately the same correlation for the environment, but *N. closterium* had a more significant relationship for DIC and DSi, while *P. globosa* had a more significant positive correlation for  $\text{N-NO}_3^-$  and TDN. Moreover, DON and DIP showed a significant positive

correlation ( $p < 0.01$ ). A significant negative correlation ( $p < 0.001$ ) was found between DSi and DIN. In addition, a significant positive correlation ( $p < 0.001$ ) existed between DOC and TDN, a significant negative correlation ( $p < 0.05$ ) was found between DOC and DON. The results indicated significant positive correlation relationships among DIC and DIN/DIP. RDA also revealed that *P. globosa* and *N. closterium* responded differently to nutrients, carbon, and environmental factors (Figure 7).

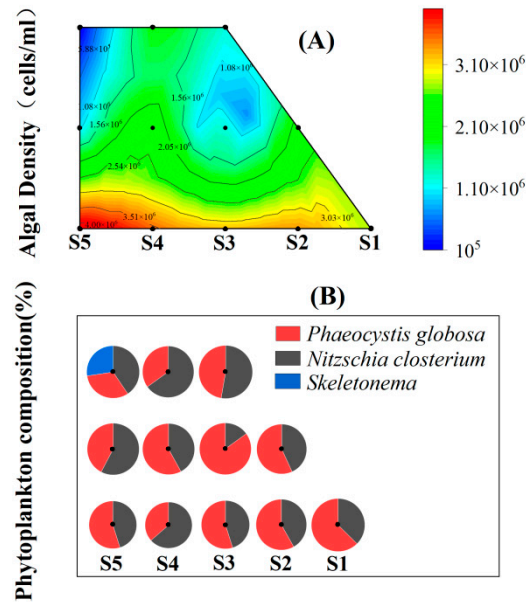


Figure 4. Spatial algal density in the JSB coastal water during spring algal bloom (A), and percentage of algae in JSB coastal waters (B).

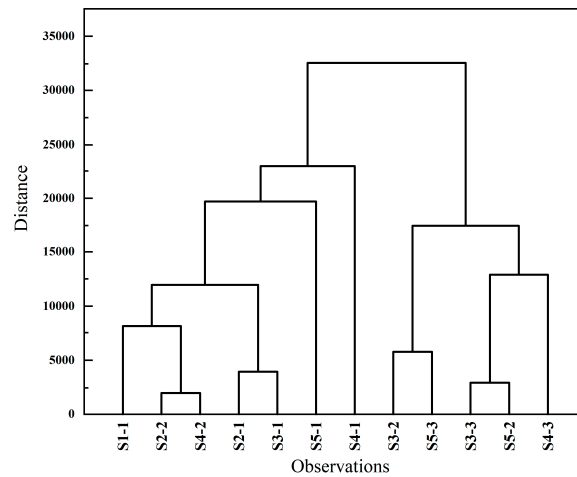
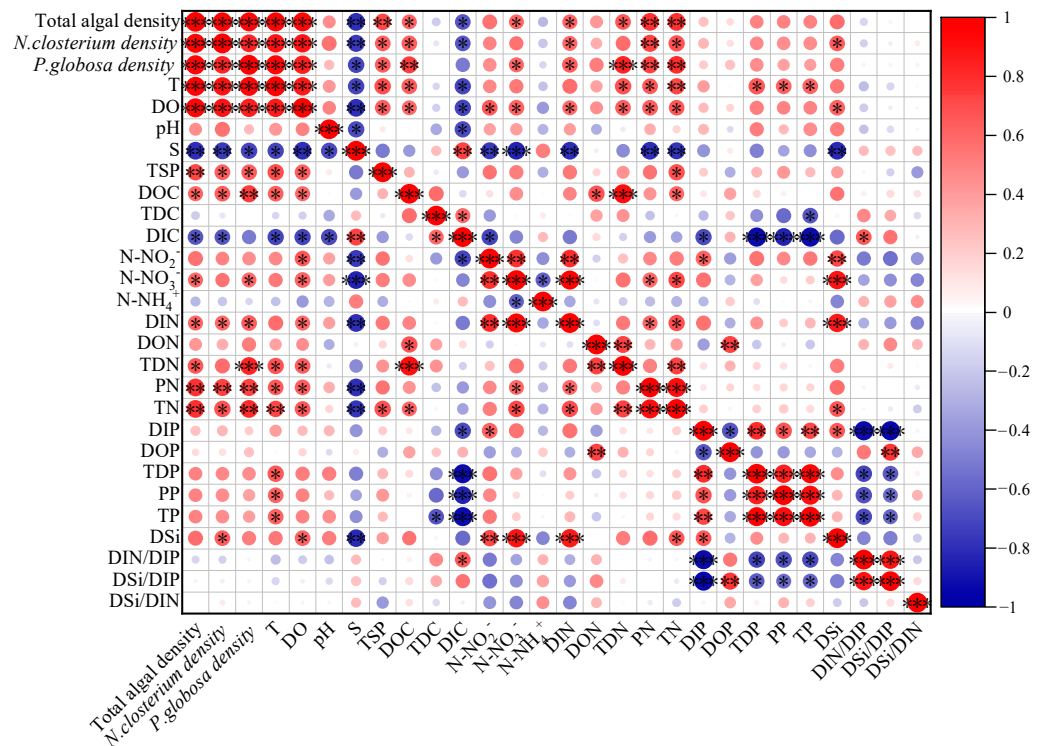
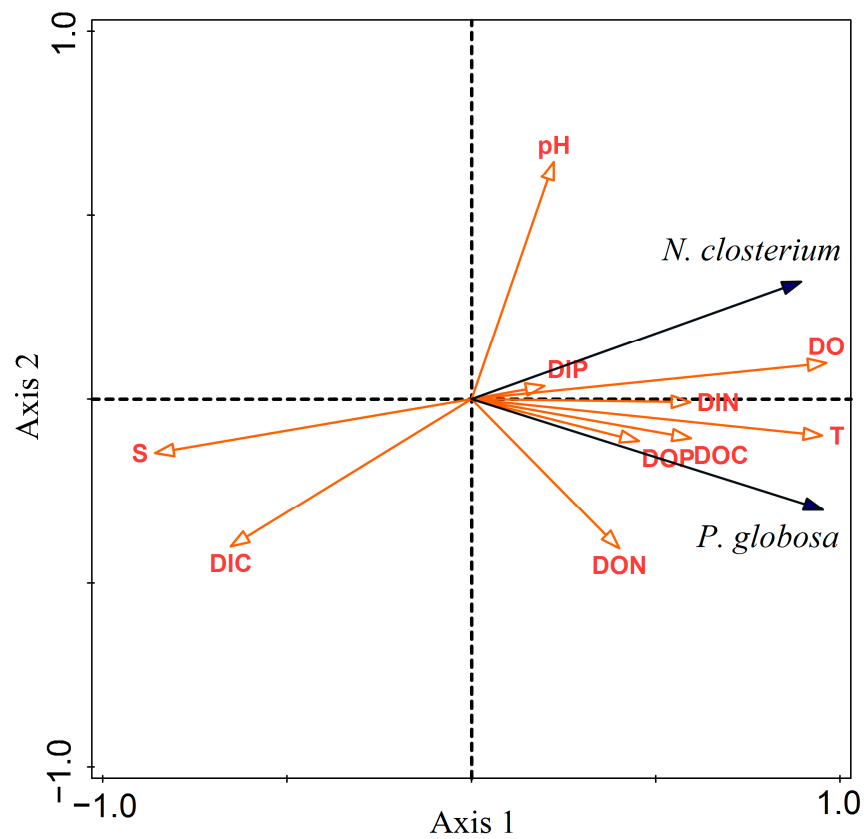


Figure 5. Cluster analysis on *Phaeocystis globosa* and *Nitzschia closterium* of JSB during spring algal bloom period.



**Figure 6.** Relationships among nutrients, carbon, and phytoplankton during spring algal bloom (n = 12, \* p < 0.05 \*\* p < 0.01 \*\*\* p < 0.001).



**Figure 7.** RDA on *P. globosa* and *N. closterium* in JSB during spring algal bloom period.

## 4. Discussion

### 4.1. Environmental Condition Induced the Phytoplankton Bloom

As an important environmental factor, T affected the metabolism and proliferation of algae directly or indirectly by influencing the enzymatic reactions of algae and the solubility of nutrients in the water column [49]. According to previous studies on the harmful algal blooms species (*P. globosa*) in the South China Sea [50], it showed that T and S had a significant effect on the growth rate of *P. globosa*. In addition, the suitable T for *P. globosa* growth ranged from 20 °C to 27 °C and the suitable S fluctuated from 20 PSU to 40 PSU [51,52]. In this survey, the average T and S in coastal water in JSB was 27.74 °C and 16.73 PSU, respectively. Therefore, the optimum T and S for algal growth induced the spring algal blooms in coastal water. This was consistent with the previous findings in Indian Sundarbans and Qinzhou Bay [53,54]. Moreover, the seawater viscosity in certain T and S was consistent with the occurrence process of *P. globosa* bloom and could be used as a valuable index for *P. globosa* bloom monitoring in Qinzhou Bay [54]. According to previous field investigations, the average pH in Zhanjiang Bay was 8.0 [55], while the average pH in this survey was 8.24, a relative increase of 0.24. According to research results, pH has a significant impact on the growth and N-NH<sub>4</sub><sup>+</sup> uptake of *N. closterium* and *Skeletonema*, and both are significantly inhibited by a decline in pH. However, the growth of the algae in the survey area may not be inhibited by pH [56,57]. The phytoplankton growth also impacts the pH and DO concentration in the coastal water [58]. During the spring algal bloom, phytoplankton has the ability to absorb DIC and releases DO through photosynthesis [59–61]. In addition, TSP showed a significant positive correlation with algal density, indicating that algae were likely to be the component of organisms in the TSP in the JSB. This was also similar to the previous findings in the northern South China Sea [62]. In summary, T was one of the causes of spring algal blooms, and during the spring algal blooms, a large amount of algae absorbed nutrients and DIC through photosynthesis and released DO, which further influenced the physicochemical properties of seawater and led to the increase of seawater pH.

### 4.2. The Interactions of Nutrients and Carbon during Spring Algal Bloom Period

In coastal systems, the “Redfield ratio” has been used to evaluate nutrient limitation [63,64]. Redfield demonstrated that the chemical composition of phytoplankton converges to an average elemental ratio of C:N:P = 106:16:1 for ocean water, and the relatively small amount of nutrients in this ratio was called limiting nutrients. Therefore, the composition of nutrients has a significant effect on phytoplankton abundance [9]. Based on the field investigation of JSB, the mean value of DIN/DIP was 6.6, which indicated that the nutrients structure of JSB seawater was imbalanced under N-limitation, and this was obviously different from previous studies on the nutrient limitation in coastal waters, for example, high DIN/DIP was found in the Yellow Sea region where algal blooms occurred [7,65]. The results showed that DIN, TN, and algal density showed a significant positive correlation, indicating that N significantly stimulated algal growth more than P during the spring algal bloom period. Furthermore, for the major spring algal bloom organisms, previous study of *P. globosa* found that the algae tolerated a wide range of P concentrations, between 0.00 μmol/L and 180.00 μmol/L. At the lower N/P, the growth rate of *P. globosa* was higher [66–68]. The nitrate reductase activity and growth rate of *P. globosa* cells increased with the increase of nitrate concentration at different nitrate concentrations, which can explain that the eutrophic sea with higher nitrate was beneficial to the continuous growth of *P. globosa* [69]. In conclusion, suitable temperature and pH also provided a good growth environment for *P. globosa* [70]. Meanwhile, nutrients stimulated the growth of algae, which played a key role in the carbon cycle, while bacteria, algae, and zooplankton form a food web that together constituted the nutrient and carbon cycling process (Figure 8) [71]. For decomposer bacteria, the decomposition of DOM was the link between bacteria and algae, which was the main source of bacterial carbon and nitrogen [72,73]. On the other hand, algae as producers were synchronized for nutrient and C uptake, and the results

indicated significant positive correlation relationships among DIC and DIN/DIP, namely the algal density was negatively correlated with DIC and positively correlated with DOC. It is suggested that phytoplankton took up DIC and nutrients through photosynthesis during the day, biosynthesized at night, and produced DOM through cleavage, passive leakage, or leaching of carbon-rich material [74–76]. Previous studies showed that the increase of carbon sources has a certain promoting effect on the population growth of *Skeletonema costatum* in the laboratory [77]. More DIC in seawater may be favorable to the algal bloom of *Skeletonema costatum*. Meanwhile, the proportion of DOC showed an increasing trend from distant shore to nearshore, in line with the distribution of algae, and DOC was positively and significantly correlated with TDN, which indicated that most of the DOM produced by algae was in the form of DOC and accompanied by the consumption and excretion of N, utilized by microzooplankton and bacteria, and the sinking phytoplankton aggregates and fecal pellets also dissolved DOC [78,79]. Zooplankton as consumers, micro- and medium-sized zooplankton ate most of the phytoplankton in seawater, and any unconsumed phytoplankton formed aggregates and zooplankton fecal pellets sank to the deeper ocean [80]. These sinking phytoplankton aggregates and feces can be consumed by the lower zooplankton, with only a small fraction entering the deep sea [18]. Therefore, the occurrence of algal blooms may accelerate the carbon sink process of the carbon cycle. These metabolites regulated the carbon cycle in marine ecosystems [81].

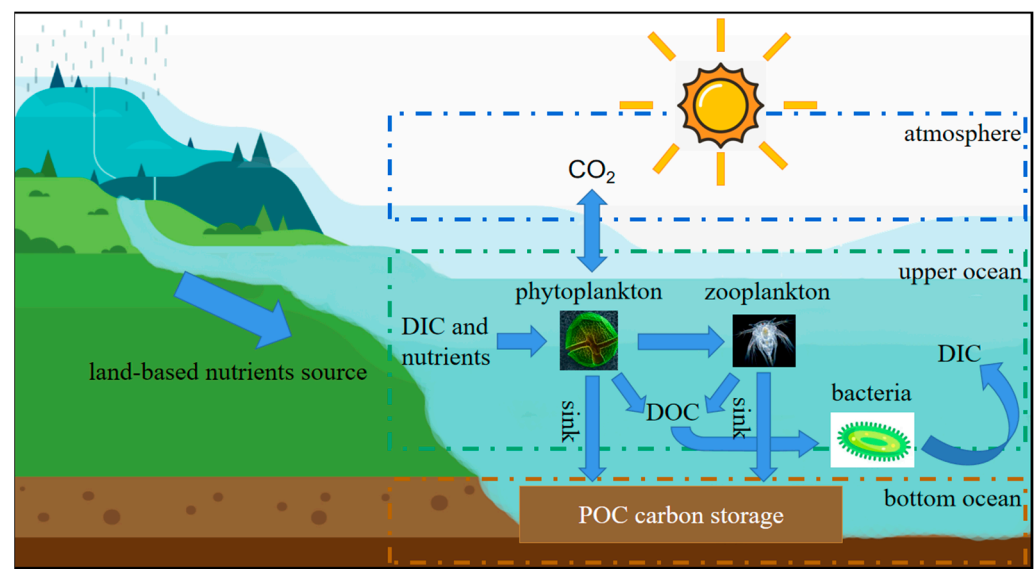


**Figure 8.** Nutrients and carbon interactions during spring algal bloom period.

#### 4.3. Mitigation Eutrophication and Preventing Spring Algal Bloom in the JSB

In previous studies in Zhanjiang Bay, the result showed that the fluxes of land-based sources of N, P to the sea in summer in Zhanjiang Bay reached 1617 t and 266 t, respectively [38]. Through the investigation of JSB, it was found that the nutrients concentration in JSB has exceeded the IV water quality standard in the Standard for Seawater Quality (GB/T3097-1997). In addition, the correlation analysis showed there was a negative correlation relationship between S and nutrients, indicating that the nutrients were mainly from land-based sources input, such as domestic wastewater and river discharge adjacent to JSB [33]. Especially, rainfall was one way of inputting pulses of nutrients; the flushing of rainwater may bring a large amount of land-based pollutants from human activities, resulting in the eutrophic status in the JSB coastal water [33]. The coastal water eutrophication provides a good environment for algal blooms to develop, which makes the occurrence of algal blooms more and more frequent. At the same time, due to the competition and predation between species, algal blooms also change the local ecological structure to a

certain extent, which in turn promotes the occurrence of algal blooms, and gets into a vicious circle. In recent years, *P. globosa* was the dominant phytoplankton species during spring in this bay [33]. In addition, from the current study, *P. globosa* and *N. closterium* phytoplankton species are present in many monitoring stations, and *H'* has decreased from 2.42 to 1.03. This indicates that algal blooms have great impact on the number and composition of phytoplankton, making phytoplankton species singleness [82]. In order to mitigate the eutrophication and prevent spring algal blooms, water T should be monitored long-term, and the discharge of nutrients, such as N and P, should be restricted in the spring season when the algal bloom is in a high frequency outbreaking period. Specifically, the deep treatment of municipal wastewater, improving the purification rate, and reducing the concentration of nutrients in the wastewater can be implemented around JSB. Moreover, in chronically eutrophic coastal water, excess nutrients are often collected by settling into the bottom sediments. When the nutrients concentration in seawater decreases, the nutrients in rich sediments in seawater may release the nutrients under the tidal variation [83]. In future research, developing an efficient, precise, and applicable early warning system for specific algal blooms, such as *P. globosa* and *N. closterium*, is urgent [54,84,85]. In addition, the physical and biogeochemical modeling and further in situ observations are needed to obtain a better understanding of the role of nutrients and carbon in spring algal bloom events. Specifically, nutrients and carbon in situ enrichment experiments and modeling should be conducted to quantitatively explore the interactions of nutrients and carbon on phytoplankton growth during the bloom period, which are implications for the reduction of land-based nutrients load and the enhancement of the marine carbon sink.

## 5. Conclusions

During the spring algal bloom in JSB in March 2022, the average TN, TP, and DSi was  $97.97 \pm 26.31 \mu\text{mol/L}$ ,  $12.84 \pm 4.48 \mu\text{mol/L}$ , and  $16.29 \pm 4.00 \mu\text{mol/L}$  in JSB, respectively. In addition, S was significantly and negatively correlated with nutrients, indicating that nutrients were mainly discharged from land-based sources. Moreover, the average concentration of TDC, DIC, and DOC in JSB was  $2187.43 \pm 195.92 \mu\text{mol/L}$ ,  $1516.25 \pm 133.24 \mu\text{mol/L}$ , and  $671.13 \pm 150.81 \mu\text{mol/L}$ , respectively. Moreover, DIC was mainly from the ocean. As the major fraction of TDC, DIC was significantly and positively correlated with S, which was mainly derived from marine sources. Furthermore, the average algal density was  $(2.20 \pm 1.24) \times 10^6$  cells/mL, and the main dominant species were *P. globosa* and *N. closterium* during the spring algal bloom. Spring algal blooms increased phytoplankton biomass density, and V level of algal blooms were reached [47]. The algal showed a significant positive correlation with T. Therefore, water T should be monitored long-term in coastal water, and the land-based nutrients sources discharge, such as N and P, should be reduced in the spring algal bloom season. Our findings revealed that nutrients and carbon interactions during the spring algal bloom period in the JSB coastal water and the large amount of phytoplankton bloom accelerated the process of DIC sinks in coastal areas. In the future research, physical and biogeochemical modeling and further in situ observations are needed to obtain better understandings of the role of nutrients and carbon in algal bloom events under climate change and anthropogenic pressures.

**Author Contributions:** Conceptualization, P.Z.; Methodology, P.Z. and J.Z.; Software, M.F.; Validation, D.S.; Formal analysis, M.F. and D.P.; data curation, M.F.; Writing—original draft preparation, P.Z., J.Z. and M.F.; Writing—review and editing, P.Z., J.Z. and M.F.; Visualization, M.F.; Supervision, J.Z.; Project administration, P.Z. and J.Z.; Funding acquisition, P.Z. and J.Z. All listed authors made substantial, direct, and intellectual contributions to the work and are approved for publication. All authors have read and agreed to the published version of the manuscript.

**Funding:** This research was funded by the Guangdong Basic and Applied Basic Research Foundation (2020A1515110483), Guangdong Basic and Applied Basic Research Foundation (2023A1515012769), Research and Development Projects in Key Areas of Guangdong Province (2020B1111020004), Guangdong Ocean University Fund Project (R18021); Science and Technology Special Project of Zhanjiang

City (2019B01081); Innovation Strong School Project (230420021) of Guangdong Ocean University for funding.

**Institutional Review Board Statement:** Not applicable.

**Informed Consent Statement:** Not applicable.

**Data Availability Statement:** Data sharing is not applicable to this article.

**Acknowledgments:** Thanks for the financial support provided by the Guangdong Basic and Applied Basic Research Foundation (2020A1515110483), Guangdong Basic and Applied Basic Research Foundation (2023A1515012769), Research and Development Projects in Key Areas of Guangdong Province (2020B1111020004), Guangdong Ocean University Fund Project (R18021); Science and Technology Special Project of Zhanjiang City (2019B01081); Innovation Strong School Project (230420021) of Guangdong Ocean University for funding. Special thanks to reviewers for their careful review and constructive suggestions. Thanks to all members of the research team and others involved in this study.

**Conflicts of Interest:** The authors declare no conflict of interest.

## References

- Conley, D.J.; Paerl, H.W.; Howarth, R.W.; Boesch, D.F.; Seitzinger, S.P.; Havens, K.E.; Lancelot, C.; Likens, G.E. Controlling eutrophication on: Nitrogen and phosphorus. *Science* **2009**, *323*, 1014–1015. [[CrossRef](#)] [[PubMed](#)]
- Howarth, R.W. Coastal nitrogen pollution: A review of sources and trends globally and regionally. *Harmful Algae* **2008**, *8*, 14–20. [[CrossRef](#)]
- Qiu, D.; Huang, L.; Zhang, J.; Lin, S. Phytoplankton dynamics in and near the highly eutrophic Pearl River Estuary, South China Sea. *Cont. Shelf Res.* **2010**, *30*, 177–186. [[CrossRef](#)]
- Lin, P.; Chen, M.; Guo, L. Speciation and transformation of phosphorus and its mixing behavior in the Bay of St. Louis estuary in the northern Gulf of Mexico. *Geochim. Cosmochim. Acta* **2012**, *87*, 283–298. [[CrossRef](#)]
- Duan, L.Q.; Song, J.M.; Yuan, H.M.; Li, X.G.; Li, N. Distribution, partitioning and sources of dissolved and particulate nitrogen and phosphorus in the north Yellow Sea. *Estuar. Coast. Shelf Sci.* **2016**, *181*, 182–195. [[CrossRef](#)]
- Zhang, P.; Xu, J.L.; Zhang, J.B.; Li, J.X.; Zhang, Y.C.; Li, Y.; Luo, X.Q. Spatiotemporal Dissolved Silicate Variation, Sources, and Behavior in the Eutrophic Zhanjiang Bay, China. *Water* **2020**, *12*, 3586. [[CrossRef](#)]
- Jin, J.; Liu, S.M.; Ren, J.L.; Liu, C.G.; Zhang, J.; Zhang, G.L. Nutrient dynamics and coupling with phytoplankton species composition during the spring blooms in the Yellow Sea. *Deep. Sea Res. Part II Top. Stud. Oceanogr.* **2013**, *97*, 16–32. [[CrossRef](#)]
- Wang, K.; Chen, J.; Jin, H.; Li, H.; Gao, S.; Lu, Y.; Weng, H. Nutrient structure and limitation in Changjiang River Estuary and adjacent East China Sea. *Acta Oceanol. Sin.* **2013**, *35*, 128–136.
- Wang, J.; Bouwman, A.F.; Liu, X.; Beusen, A.H.; Van Dingenen, R.; Dentener, F.; Yao, Y.; Glibert, P.M.; Ran, X.; Yao, Q.; et al. Harmful algal blooms in Chinese coastal waters will persist due to perturbed nutrient ratios. *Environ. Sci. Technol. Lett.* **2021**, *8*, 276–284. [[CrossRef](#)]
- Cotner, J.B.; Biddanda, B.A. Small players, large role: Microbial influence on biogeochemical processes in pelagic aquatic ecosystems. *Ecosystems* **2002**, *5*, 105–121. [[CrossRef](#)]
- Zhang, P.; Peng, C.H.; Zhang, J.B.; Zou, Z.B.; Shi, Y.Z.; Zhao, L.R.; Zhao, H. Spatiotemporal urea distribution, sources, and indication of DON bioavailability in Zhanjiang Bay, China. *Water* **2020**, *12*, 633. [[CrossRef](#)]
- Kang, Y.; Kang, C.K. Reduced forms of nitrogen control the spatial distribution of phytoplankton communities: The functional winner, dinoflagellates in an anthropogenically polluted estuary. *Mar. Pollut. Bull.* **2022**, *177*, 113528. [[CrossRef](#)] [[PubMed](#)]
- Tyrrell, T. The relative influences of nitrogen and phosphorus on oceanic primary production. *Nature* **1999**, *400*, 525–531. [[CrossRef](#)]
- Cai, W.J. Estuarine and coastal ocean carbon paradox: CO<sub>2</sub> sinks or sites of terrestrial carbon incineration? *Annu. Rev. Mar. Sci.* **2011**, *3*, 123–145. [[CrossRef](#)]
- Li, X.; Liu, Z.; Chen, W.; Wang, L.; He, B.; Wu, K.; Gu, S.; Jiang, P.; Huang, B.; Dai, M. Production and transformation of dissolved and particulate organic matter as indicated by amino acids in the Pearl River Estuary, China. *J. Geophys. Res. Biogeosci.* **2018**, *123*, 3523–3537. [[CrossRef](#)]
- Kubo, A.; Kanda, J. Coastal urbanization alters carbon cycling in Tokyo Bay. *Sci. Rep.* **2020**, *10*, 20413. [[CrossRef](#)]
- Ittekkot, V. Variations of dissolved organic matter during a plankton bloom: Qualitative aspects, based on sugar and amino acid analyses. *Mar. Chem.* **1982**, *11*, 143–158. [[CrossRef](#)]
- Bauer, J.E.; Cai, W.J.; Raymond, P.A.; Bianchi, T.S.; Hopkinson, C.S.; Regnier, P.A. The changing carbon cycle of the coastal ocean. *Nature* **2013**, *504*, 61–70. [[CrossRef](#)]
- Kuwae, T.; Kanda, J.; Kubo, A.; Nakajima, F.; Ogawa, H.; Sohma, A.; Suzumura, M. CO<sub>2</sub> uptake in the shallow coastal ecosystems affected by anthropogenic impacts: Carbon dynamics, policy, and implementation. In *Blue Carbon in Shallow Coastal Ecosystems*; Kuwae, T., Hori, M., Eds.; Springer: Singapore, 2019; pp. 295–319.

20. Hopkinson, C.S., Jr.; Vallino, J.J.; Nolin, A. Decomposition of dissolved organic matter from the continental margin. *Deep Sea Res. Part II Top. Stud. Oceanogr.* **2002**, *49*, 4461–4478. [[CrossRef](#)]
21. Bricker, S.B.; Longstaff, B.; Dennison, W.; Jones, A.; Boicourt, K.; Wicks, C.; Woerner, J. Effects of nutrient enrichment in the nation's estuaries: A decade of change. *Harmful Algae* **2008**, *8*, 21–32. [[CrossRef](#)]
22. Wang, Y.; Liu, D.; Xiao, W.; Zhou, P.; Tian, C.; Zhang, C.; Wang, B. Coastal eutrophication in China: Trend, sources, and ecological effects. *Harmful Algae* **2021**, *107*, 102058. [[CrossRef](#)] [[PubMed](#)]
23. Zhang, P.; Luo, W.; Fu, M.; Zhang, J.; Cheng, M.; Xie, J. Effects of tidal variations on total nitrogen concentration, speciation, and exchange flux in the Shuidong Bay coastal water, South China Sea. *Front. Mar. Sci.* **2022**, *9*, 961560. [[CrossRef](#)]
24. Lin, G.; Lin, X. Bait input altered microbial community structure and increased greenhouse gases production in coastal wetland sediment. *Water Res.* **2022**, *218*, 118520. [[CrossRef](#)] [[PubMed](#)]
25. Zhang, J.B.; Zhang, P.; Dai, P.D.; Lai, J.Y.; Chen, Y. Spatiotemporal distributions of DIP and the eutrophication in Hainan Island adjacent coastal water. *Zhongguo Huanjing Kexue China Environ. Sci.* **2019**, *39*, 2541–2548.
26. Yang, B.; Kang, Z.J.; Lu, D.L.; Dan, S.F.; Ning, Z.M.; Lan, W.L.; Zhong, Q.P. Spatial variations in the abundance and chemical speciation of phosphorus across the river–Sea interface in the Northern Beibu Gulf. *Water* **2018**, *10*, 1103. [[CrossRef](#)]
27. Huang, F.; Lin, X.; Hu, W.; Zeng, F.; He, L.; Yin, K. Nitrogen cycling processes in sediments of the Pearl River Estuary: Spatial variations, controlling factors, and environmental implications. *Catena* **2021**, *206*, 105545. [[CrossRef](#)]
28. Wei, Q.; Yao, Q.; Wang, B.; Wang, H.; Yu, Z. Long-term variation of nutrients in the southern Yellow Sea. *Cont. Shelf Res.* **2015**, *111*, 184–196. [[CrossRef](#)]
29. Sun, F.; Wang, C.; Wang, Y.; Tu, K.; Zheng, Z.; Lin, X. Diatom red tide significantly drive the changes of microbiome in mariculture ecosystem. *Aquaculture* **2020**, *520*, 734742. [[CrossRef](#)]
30. Davidson, K.; Gowen, R.J.; Harrison, P.J.; Fleming, L.E.; Hoagland, P.; Mosconas, G. Anthropogenic nutrients and harmful algae in coastal waters. *J. Environ. Manag.* **2014**, *146*, 206–216. [[CrossRef](#)]
31. Wei, Q.; Wang, B.; Yao, Q.; Yu, Z.; Fu, M.; Sun, J.; Xin, M. Physical-biogeochemical interactions and potential effects on phytoplankton and *Ulva prolifera* in the coastal waters off Qingdao (Yellow Sea, China). *Acta Oceanol. Sin.* **2019**, *38*, 11–23. [[CrossRef](#)]
32. Zhang, J.; Yang, Y.; Yang, L.; Li, J.R.; Zhang, Y.Q. Relationship between red tide occurrence and environmental factors in offshore waters of East China Sea. *J. Guangdong Ocean Univ.* **2019**, *39*, 66–70.
33. Zhang, P.; Peng, C.; Zhang, J.; Zhang, J.; Chen, J.; Zhao, H. Long-term harmful algal blooms and nutrients patterns affected by climate change and anthropogenic pressures in the Zhanjiang Bay, China. *Front. Mar. Sci.* **2022**, *9*, 849819. [[CrossRef](#)]
34. Wang, B. Cultural eutrophication in the Changjiang (Yangtze River) plume: History and perspective. *Estuar. Coast. Shelf Sci.* **2006**, *69*, 471–477. [[CrossRef](#)]
35. Li, B.H.; Hu, J.W.; Xin, Y.; Liu, C.Y.; Li, P.F.; Yang, G.P. Changes in dissolved organic pool and regulation of associated nutrients during green tides: A case study of *Ulva prolifera* bloom in the southern Yellow Sea. *Sci. Total Environ.* **2022**, *838*, 155878. [[CrossRef](#)] [[PubMed](#)]
36. Greening, H.; Janicki, A.; Sherwood, E.T.; Pribble, R.; Johansson, J.O.R. Ecosystem responses to long-term nutrient management in an urban estuary: Tampa Bay, Florida, USA. *Estuar. Coast. Shelf Sci.* **2014**, *151*, A1–A16. [[CrossRef](#)]
37. Desmit, X.; Thieu, V.; Billen, G.; Campuzano, F.; Dulière, V.; Garnier, J.; Lassaletta, L.; Ménesguen, A.; Neves, R.; Pinto, L.; et al. Reducing marine eutrophication may require a paradigmatic change. *Sci. Total Environ.* **2018**, *635*, 1444–1466. [[CrossRef](#)] [[PubMed](#)]
38. Zhang, P.; Wei, L.R.; Jin, Y.L.; Dai, P.D.; Chen, Y.; Zhang, J.B. Concentration, composition and fluxes of land-based nitrogen and phosphorus source pollutants input into Zhanjiang Bay in summer. *J. Guangdong Ocean Univ.* **2019**, *39*, 46–55.
39. Yuan, Q.; Xu ZYPeng, H.Q.; Lu, J.M.; Huang, L.C.; Liang, X.J.; Mo, Y.Y.; Liang, Q.L. Research on nitrogen and phosphorus variation trend in Zhanjiang Harbor and its near waters in recent five years. *J. Green Sci. Technol.* **2016**, *24*, 41–45.
40. Guan, L.J.; Liao, J. Zhanjiang harbor: Bay remediation for a new look. *Ocean Fish.* **2018**, *4*, 30–32.
41. GB3838-2002; Environmental Quality Standards for Surface Water. Ministry of Environment Protection, People's Republic of China, Standards Press of China: Beijing, China, 2002.
42. GB 17378.4-2007; The Specification of Oceanographic Survey-Part 4: Survey of Chemical Parameters in Sea Water. China National Standardization Management Committee: Beijing, China, 2007.
43. Grasshoff, K.; Kremling, K.; Ehrhardt, M. (Eds.) *Methods of Seawater Analysis*; John Wiley & Sons: Hoboken, NJ, USA, 2009.
44. Yang, G.P.; Zhang, Y.P.; Lu, X.L.; Ding, H.B. Distributions and seasonal variations of dissolved carbohydrates in the Jiaozhou Bay, China. *Estuar. Coast. Shelf Sci.* **2010**, *88*, 12–20. [[CrossRef](#)]
45. GB/T 12763.6-2007; Specifications for Oceanographic Survey-Part 6: Marine Biological Survey. China National Standardization Management Committee: Beijing, China, 2007.
46. Wen, J. *Atlas of Common Freshwater Planktonic Algae in China*; Shanghai Scientific & Technical Publishers: Shanghai, China, 2010.
47. Guangdong Market Supervision Administration. *Technical Specification for Classification and Monitoring of Algal Blooms*; Guangdong Market Supervision Administration: Shenzhen, China, 2020.
48. China National Standardization Management Committee. *Specification for Marine Monitoring-Part 7: Ecological Survey for Offshore Pollution and Biological Monitoring*; China National Standardization Management Committee: Beijing, China, 2007.

49. Weng, C.S.; Liu, D.F.; Zhang, J.L.; Gong, C.; Shen, X.Z. Influence of Rainfall on the In-Situ Growth of Dominant Algae Species in Xiangxi River. *Environ. Sci.* **2019**, *40*, 3108–3117. [[CrossRef](#)]
50. Shen, P.P.; Qi, Y.Z.; Ou, L.J. *Phaeocystis globosa* in coastal China: Taxonomy, distribution, and its blooms. *Mar. Sci.* **2018**, *10*, 146–162.
51. Xu, N. Ecological Niche of Typical Red Tide Algae along the Chinese Coast. Ph.D. Dissertation, Jinan University, Guangzhou, China, 2006.
52. Xu, N.; Huang, B.Z.; Hu, Z.X.; Tang, Y.Z.; Duan, S.S.; Zhang, C.W. Effects of temperature, salinity, and irradiance on the growth of harmful algal bloom species *Phaeocystis globosa* Scherffel (*Prymnesiophyceae*) isolated from the South China Sea. *Chin. J. Oceanol. Limnol.* **2017**, *35*, 557–565. [[CrossRef](#)]
53. Sekh, S.; Biswas, B.; Mandal, M.; Sarkar, N.S. Seasonal dynamics of the genus: Planktoniella Schutt in the estuarine waters of Indian Sundarbans. *SpringerPlus* **2016**, *5*, 611. [[CrossRef](#)] [[PubMed](#)]
54. Kang, Z.J.; Yang, B.; Lai, J.X.; Ning, Y.; Zhong, Q.P.; Lu, D.L.; Liao, R.Q.; Wang, P.; Dan, S.F.; She, Z.C.; et al. *Phaeocystis globosa* bloom monitoring: Based on *P. globosa* induced seawater viscosity modification adjacent to a nuclear power plant in Qinzhou Bay, China. *J. Ocean Univ. China* **2020**, *19*, 1207–1220. [[CrossRef](#)]
55. Zhou, M.; Zhao, H. Spatio-temporal Distribution of Chl-a Concentration in Sea Surface and Its Correlation with Environmental Factors of Zhanjiang Bay in Autumn. *J. Guangdong Ocean Univ.* **2021**, *41*, 25–35.
56. Li, K.; Li, M.; He, Y.; Gu, X.; Lu, D. Effects of pH and nitrogen form on nitzschia closterium growth by linking dynamic with enzyme activity. *Chemosphere* **2020**, *249*, 126154. [[CrossRef](#)]
57. Gu, X.; Li, K.; Pang, K.; Ma, Y.; Wang, X. Effects of pH on the growth and NH<sub>4</sub>-N uptake of skeletonema costatum and nitzschia closterium. *Mar. Pollut. Bull.* **2017**, *124*, 946–952. [[CrossRef](#)]
58. Shi, Y.Z.; Zhao, H.; Wang, X.D.; Zhang, J.B.; Sun, X.L.; Yang, G.H. Distribution Characteristics of Nutritive Salts and Chlorophyll a in the Pearl River Estuary. *J. Guangdong Ocean Univ.* **2019**, *39*, 56–65.
59. Ji, Y.; Gao, K. Effects of climate change factors on marine macroalgae: A review. *Adv. Mar. Biol.* **2021**, *88*, 91–136. [[CrossRef](#)]
60. Jarvie, H.P.; Love, A.J.; Williams, R.J.; Neal, C. Measuring in-stream productivity: The potential of continuous chlorophyll and dissolved oxygen monitoring for assessing the ecological status of surface waters. *Water Sci. Technol.* **2003**, *48*, 191–198. [[CrossRef](#)]
61. Sun, X.H.; Li, Z.; Ding, X.Y.; Ji, G.L.; Wang, L.; Gao, X.T.; Chang, Q.G.; Zhu, L.X. Effects of Algal Blooms on Phytoplankton Composition and Hypoxia in Coastal Waters of the Northern Yellow Sea, China. *Front. Mar. Sci.* **2022**, *9*, 897418. [[CrossRef](#)]
62. Huang, C.; Lao, Q.; Chen, F.; Zhang, S.; Chen, C.; Bian, P.; Zhu, Q. Distribution and Sources of Particulate Organic Matter in the Northern South China Sea: Implications of Human Activity. *J. Ocean Univ. China* **2021**, *20*, 1136–1146. [[CrossRef](#)]
63. Redfield, A.C.; Ketchum, B.H.; Richards, F.A. The Influence of Organisms on the Composition of Sea Water. In *The Seas; The Composition and Descriptive Oceanography*; Hill, M.N., Ed.; Interscience Publilation: New York, NY, USA, 1963; Volume 2.
64. Davidson, K.; Flynn, K.J.; Cunningham, A. Non-steady state ammonium-limited growth of the marine phytoflagellate, *Isochrysis galbana* Parke. *New Phytol.* **1962**, *122*, 433–438. [[CrossRef](#)] [[PubMed](#)]
65. Glibert, P.M.; Seitzinger, S.P.; Heil, C.A.; Burkholder, J.M.; Parrow, M.W.; Codispoti, L.A.; Vince, K. The role of eutrophication in the global proliferation of harmfuls. *Oceanography* **2005**, *18*, 198–209. [[CrossRef](#)]
66. Guo, J.; Yang, W.D.; Liu, J.S.; Fan, Z.H. Effects of salinity, temperature and light intensity on the growth and toxin production of *Phaeocystis globosa*. *Acta Sci. Circumstantiae* **2007**, *27*, 1341–1346.
67. Chen, J.F.; Xu, N.; Jiang, T.J. A report of *Phaeocystis globosa* bloom in coastal water of southeast China. *J. Jinan Univ.* **1999**, *20*, 124–129.
68. Xu, M.B.; Zhang, R.C.; Jiang, F.J.; Pan, H.Z.; Li, J.; Yu, K.F.; Lai, J.X. Spatiotemporal Variation in Phytoplankton and Physiochemical Factors during *Phaeocystis globosa* Red-Tide Blooms in the Northern Beibu Gulf of China. *Water* **2022**, *14*, 1099. [[CrossRef](#)]
69. Wang, Y.; Tang, H.; Jiang, L.; Li, S. Effects of nitrate on the growth and nitrate reductase activity in *Phaeocystis globosa*. *Chin. Bull. Bot.* **2006**, *23*, 138.
70. Riegman, R.; Van Boekel, W. The ecophysiology of *Phaeocystis globosa*: A review. *J. Sea Res.* **1996**, *35*, 235–242. [[CrossRef](#)]
71. Sterner, R.W.; Elser, J.J. books and arts-Ecological Stoichiometry: The Biology of Elements from Molecules to the Biosphere-Reviewed by David W Schindler. *Nature* **2003**, *423*, 225.
72. Wheeler, P.A.; Kirchman, D.L. Utilization of inorganic and organic nitrogen by bacteria in marine systems 1. *Limnol. Oceanogr.* **1986**, *31*, 998–1009. [[CrossRef](#)]
73. Kirchman, D.L. The uptake of inorganic nutrients by heterotrophic bacteria. *Microb. Ecol.* **1994**, *28*, 255–271. [[CrossRef](#)] [[PubMed](#)]
74. Anderson, T.R.; Williams, P.L.B. Modelling the seasonal cycle of dissolved organic carbon at Station E1 in the English Channel. *Estuar. Coast. Shelf Sci.* **1998**, *46*, 93–109. [[CrossRef](#)]
75. Wada, M.; Takano, Y.; Nagae, S.; Ohtake, Y.; Umezawa, Y.; Nakamura, S.; Yoshida, M.; Matsuyama, Y.; Iwataki, M.; Takeshita, S.; et al. Temporal dynamics of dissolved organic carbon (DOC) produced in a microcosm with red tide forming algae *Chattonella marina* and its associated bacteria. *J. Oceanogr.* **2018**, *74*, 587–593. [[CrossRef](#)]
76. Zhou, Y.; Wang, X.; Wang, W.B.; Xu, H.Q.; Wang, S.J.; Dou, S.J.; Yang, M.; Li, L.Y.; Liu, G.Z. Establishment and Characterization of a Outdoor Open Culture System for Microalgae *Chlorella sorokiniana*. *J. Guangdong Ocean Univ.* **2021**, *41*, 33–40.
77. Liu, Z.Y.; Qi, S.B.; He, N.; Kou, J.F.; Sun, K.F. Effects of nitrogen, phosphorus and carbon on growth of seven marine microalgae. *South China Fish. Sci.* **2020**, *16*, 87–97. [[CrossRef](#)]
78. Cohen, N.R. Mixotrophic plankton foraging behaviour linked to carbon export. *Nat. Commun.* **2022**, *13*, 1302. [[CrossRef](#)]

79. Asmala, E.; Haraguchi, L.; Jakobsen, H.H.; Massicotte, P.; Carstensen, J. Nutrient availability as major driver of phytoplankton-derived dissolved organic matter transformation in coastal environment. *Biogeochemistry* **2018**, *137*, 93–104. [[CrossRef](#)]
80. Sun, J. Marine phytoplankton and biological carbon sinks. *Acta Ecol. Sin.* **2011**, *31*, 5372–5378.
81. Zhao, W.; Zhuo, P. Dissolved organic matter and its role in red tide succession in the East China Sea in spring. *Chin. J. Oceanol. Limnol.* **2011**, *29*, 795–799. [[CrossRef](#)]
82. Ma, Q.M.; Yang, F. Level of eutrophication and phytoplankton diversity in zhanjiang bay. *Trans. Oceanol. Limnol.* **2009**, *3*, 121–126. [[CrossRef](#)]
83. Berthold, M.; Schumann, R. Phosphorus dynamics in a eutrophic lagoon: Uptake and utilization of nutrient pulses by phytoplankton. *Front. Mar. Sci.* **2020**, *7*, 281. [[CrossRef](#)]
84. Wang, J.; Wang, Y.; Lai, J.; Li, J.; Yu, K. Improvement and application of qPCR assay revealed new insight on early warning of *Phaeocystis globosa* bloom. *Water Res.* **2022**, *229*, 119439. [[CrossRef](#)] [[PubMed](#)]
85. Guan, W.; Bao, M.; Lou, X.; Zhou, Z.; Yin, K. Monitoring, modeling and projection of harmful algal blooms in China. *Harmful Algae* **2022**, *111*, 102164. [[CrossRef](#)]

**Disclaimer/Publisher's Note:** The statements, opinions and data contained in all publications are solely those of the individual author(s) and contributor(s) and not of MDPI and/or the editor(s). MDPI and/or the editor(s) disclaim responsibility for any injury to people or property resulting from any ideas, methods, instructions or products referred to in the content.